Radioprotection 2021, 56(2), 111–115

https://doi.org/10.1051/radiopro/2021006

Available online at:
www.radioprotection.org

ARTICLE

Ionizing radiation and its considerations in imaging diagnosis: comparison of absorbed dose between cone beam computed tomography and multi-detector computed tomography in the head and neck

P.L.E. Oliveira[1,*], C.R. Starling[1], C.L.P. Maurício[2], F.R. Guedes[3], M.A. Visconti[3] and A.C.O. Ruellas[1,4]

[1] Department of Orthodontics and Pediatric Dentistry, Universidade Federal do Rio de Janeiro, Rio de Janeiro, Brazil.
[2] Graduate program in Radioprotection and Dosimetry, Instituto de Radioproteção e Dosimetria (IRD), Rio de Janeiro, Rio de Janeiro, Brazil.
[3] Department of Pathology and Oral Radiology, Universidade Federal do Rio de Janeiro, Rio de Janeiro, Brazil.
[4] Department of Orthodontics and Pediatric Dentistry, University of Michigan, Ann Arbor, MI, USA.

Received: 31 May 2020 / Accepted: 11 March 2021

Abstract – *Introduction:* The objective of this study was to compare the mean absorbed dose in patients undergoing head and neck examinations using two cone beam computed tomography (CBCT, Kodak and i-CAT) and one multi-detector computed tomography (MDCT). *Methods:* Three thermoluminescent dosimeters (TLDs), calibrated in air kerma, were positioned in 24 regions of the head and neck of a phantom simulating an average adult. The mean absorbed dose (mGy) values in these positions, for different organs and tissues, were obtained using correction factors, considering the ratio between the mass energy absorption coefficients of organ/tissue and air. Comparison between radiation doses in the most radiosensitive regions was done by calculating the ratio of these dose values, with propagated uncertainty. *Results:* The dose in all regions was significantly higher for MDCT when compared to CBCT. Concerning CBCT equipment, the Kodak device had a higher absorbed dose than the i-CAT for most of the regions tested. The uncertainty of the i-CAT was greater than that of the Kodak. *Conclusion:* Due to the considerable difference between absorbed doses, emphasizing the higher dose values obtained in MDCT, the dissemination of CBCT application in medicine is recommended, as well as further studies to broaden the criteria for use.

Keywords: radiation protection / cone-beam computed tomography / multidetector computed tomography / absorption / radiation / radiation dosimeters

1 Introduction

Cone beam computed tomography (CBCT) is a diagnostic resource introduced in the last two decades (Hodez *et al.*, 2011). It is a very useful exam in dentomaxillofacial diagnosis, orthodontic treatment and surgical planning, for example, for risk assessment in the extraction of third molars (Sun *et al.*, 2017; Hodez *et al.*, 2011; Loubele *et al.*, 2009). In medicine, the frequency of requesting CBCT scans is unknown; nevertheless, its application is possible, especially in otorhinolaryngology (Xu *et al.*, 2012; Razafindranaly *et al.*, 2016; Ruivo *et al.*, 2009). It is noteworthy that application and acceptance of CBCT are limited due to lower image quality in relation to multi-detector computed tomography (MDCT) (Loubele *et al.*, 2009).

MDCT is high-quality exam for several health conditions and can benefit patients on adoption of the correct criteria (Xu *et al.*, 2012). In addition, it is important to investigate scan protocols for the head and neck with the CBCT technique to compare radiation doses between the types of computed tomography. Thus, understanding the absorbed dose, type and quality of image generated, it is possible to protect the patient from the effects of ionizing radiation and establish radiodiagnosis based on ALARA principles.

The aim of this study was to compare the mean absorbed dose in a receptor undergoing a head and neck exam with two CBCT scanners and one MDCT.

*Corresponding author: pedroemmerich@hotmail.com

2 Methods and materials

2.1 Study sample and design

To conduct the experiment, an Alderson Rando Phantom (Alderson Research Laboratories, NY, USA; Fig. 1) was used, simulating an average adult (1.75 m tall), with LiF : Mg, Cu, P (TLD100H) and LiF : Mg, Ti (TLD100) thermoluminescent dosimeter (TLD) chips, individually calibrated in air kerma free in air in a standardized Caesium-137 beam traced to the Brazilian National Metrology of Ionizing Radiation. All TLDs were read in a Harshaw 5500 Series semi-automatic reader (Harshaw/Bicron, Solon, OH, USA). TLD100H was applied at MDCT and TLD100 at CBCT because they are effective dosimeters for dosimetry in high and low dose fields respectively.

TLD100 chips were annealed in a TLDO automatic oven before each irradiation at 400 °C for 1 h, followed by 100 °C for 2 h and, before each reading, preheated in the same oven at 100 °C for 10 min. All readings were done with a linear heating hate of 15 °C/s from 100 °C to 350 °C, and the acquisition time was 20 s. The TLD100H chips were not treated in the oven. Their readings were done after a preheat of 10 s at 145 °C and with a linear temperature rate of 23 1/3 s from 145 °C to 260 °C. After the readings, the TLD100H chips were annealed in the reader at 145 °C for 10 s.

After calibration of the dosimeters, they were positioned in 24 regions of the phantom, by the same operator to avoid positioning errors, considered radiosensitive in the human head and neck (Tab. 1 and Fig. 1), going from the lens to the thyroid gland. The areas were selected based on previous studies (Ludlow and Walker 2013; Ludlow *et al.*, 2006; Chinem *et al.*, 2016). In each area, three dosimeters were placed to obtain the mean dose.

The tomography was obtained with Kodak K9500® (Carestream Health, Rochester, NY, USA), i-CAT® (Imaging Sciences International, Hartfield, PA, USA) and PET/CT Optima 560 GE scanners. The equipment was calibrated with the standard parameters described in Table 2 and the field of view required to cure the skull and face.

2.2 Calculation of doses

All dosimeters were reset to zero before the experiments and travel dosimeters, with the same environmental and displacement conditions as the test dosimeters, were used to eliminate energy other than from computed tomography devices. To obtain the mean absorbed dose in organs and tissues, correction factors were used considering the ratio of the mass energy absorption coefficient $\frac{\mu en}{\rho}$ of the organ/tissue and air, as described in Table 3.

2.3 Data analysis

The mean values and standard deviation(s) were calculated for each TLD position in tissues. Then, the type A uncertainty of the mean value was calculated for 95% confidence level ($I_{95\%}$) considering n of 3, and $t_{3.95\%}$, according to the equation below:

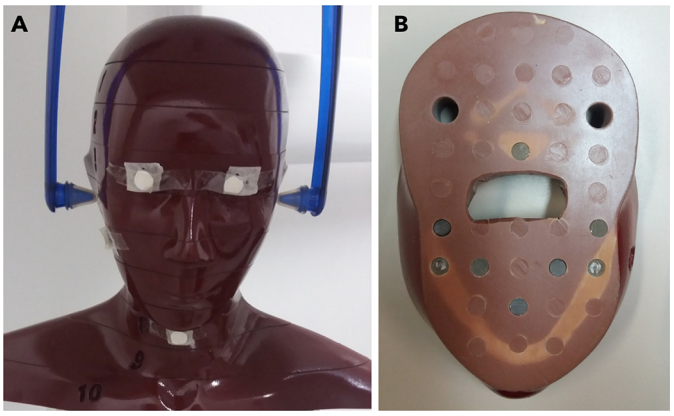

Fig. 1. A and B) Phantom with positioned TLDs.

$$I_{95\%} = \frac{t_{3.95\%} \times s}{\sqrt{3}} = \frac{4.3 \times s}{\sqrt{3}}.$$

To compare radiation doses in the more radiosensitive regions, the ratio of the mean values was also calculated between the three types of tomograph with their propagated uncertainty, according to the equations below. While x and y represent the average dose absorbed in the tissues and Ix and Iy the uncertainty for the MDCT, I-cat or Kodak devices.

Ratio of means: $\frac{x}{y}$.

Propagation of uncertainty: $I\left(\frac{x}{y}\right) = \frac{x}{y}\sqrt{\left(\frac{Ix}{x}\right)^2 + \left(\frac{Iy}{y}\right)^2}$.

3 Results

3.1 Average absorbed dose at dosimeter sites

Table 1 presents the mean absorbed dose values for each organ/tissue position measured with the TLD (in mGy), after correction using the mass energy absorption factor ratio. The absorbed dose values obtained with MDCT were significantly higher at all dosimeter sites than those obtained with CBCT equipment. In the middle of the thyroid, a value of 60.33 mGy was observed; in the mandibular body, the highest values were 74.24 and 75.09 mGy. Kodak equipment presented a greater absorbed dose than i-CAT at most sites; however, the opposite occurred in the middle of the thyroid. The uncertainty of the i-CAT, in general, was higher than that of the Kodak, that is, a greater variation between the readings of the three dosimeters in the same area. In the centre of the cervical spine, for example, it was scored as 2.12 (mean dosed absorbed) with 0.20 of uncertainty for the Kodak, and 1.84 (mean absorbed dose) with 0.64 of uncertainty for the i-CAT.

3.2 Ratio and propagation of uncertainty between MDCT and CBCT

In regions with higher radiosensitivity, MDCT presented scores 13 times greater than the Kodak and 17 times greater than the i-CAT in the left and right eye lenses. In the thyroid surface dosimeter, the MDCT dose reached 150 times that of the CBCT. In glandular regions, the dose for MDCT ranged from 17 to 25 times greater than for CBCT. The midline thyroid also presented higher scores, with an absorbed dose for MDCT 30 times greater than for the i-CAT and 67 times greater than for the Kodak (Tab. 4).

Table 1. Mean tissue absorbed dose at each TLD position (mGy), and uncertainty at 95% confidence level (between parentheses).

Material	Dosimeter location	Position of TLDs	CBCT Kodak	CBCT I-cat	MDCT
Bone	Anterior calvarium	1	4.66 (0.07)	2.34 (0.17)	60.15 (3.20)
	Posterior calvarium	2	4.07 (0.12)	2.05 (0.27)	41.39 (2.06)
	Left calvarium	3	3.44 (0.07)	2.38 (0.17)	56.17 (3.87)
	Right ramus	5	4.88 (0.12)	2.82 (0.15)	65.88 (1.79)
	Left ramus	6	5.48 (0.37)	2.84 (0.42)	71.20 (6.83)
	Right mandibular body	7	5 (0.44)	2.83 (0.84)	75.09 (15.73)
	Left mandibular body	8	5.95 (0.59)	2.82 (0.47)	74.24 (5.99)
	Center of cervical spine	4	2.12 (0.20)	1.84 (0.62)	47.08 (1.86)
Soft tissue	Middle of the brain	9	1.98 (0.22)	1.74 (0.24)	37.29 (4.10)
	Pituitary fossa	10	1.66 (0.15)	2.07 (0.15)	30.13 (3.48)
	Right orbit	11	2.59 (0.12)	2.47 (0.57)	39.21 (1.66)
	Left orbit	12	2.44 (0.12)	2.37 (0.39)	39.93 (3.15)
	Right eye lens*	13	2.76 (0.15)	2.18 (0.64)	37.99 (4.40)
	left eye lens*	14	2.67 (0.27)	2.12 (0.67)	36.82 (1.86)
	Right parotid Gl	15	2.65 (0.07)	1.97 (0.09)	46.66 (5.39)
	Left parotid Gl	16	2.78 (0.09)	1.98 (0.17)	49.91 (6.51)
	Right submandibular Gl	17	2.42 (0.17)	1.82 (0.07)	44.31 (3.80)
	Left submandibular Gl	18	2.73 (0.57)	1.94 (0.62)	42.43 (2.33)
	Sublingual Gl	19	2.35 (0.15)	1.80 (0.17)	44.38 (1.04)
	Thyroid surface*	20	0.4 (0.05)	0.41 (0.07)	60.08 (6.09)
	Midline thyroid	21	0.89 (0.09)	2 (0.24)	60.33 (3.55)
	Right cheek*	22	2.44 (0.20)	1.55 (0.09)	37.69 (4.99)
	Left back of neck	23	1.32 (0.20)	1.19 (0.24)	35.98 (4.00)
Air	Naso-pharyngeal air space	24	0.34 (0.02)	0.36 (0.15)	51.18 (7.10)

Gl: Gland.
* Surface dosimeters.

Table 2. Parameters adopted.

Equipment	FOV	kVp	mA	Time (s)
KODAK K9500® (Carestream Health, Rochester, USA)	18 cm	90	10	10.8
I-Cat® (Imaging Sciences International, Hatfield, Pennsylvania, USA)	22 cm	120	1.84	40
PET/CT Optima 560 GE	–	120	80	22.6

FOV: field of view; kVp: kilovoltage peak; mA: miliampers.

Table 3. Ratio of mass energy absorption coefficients applied for calculation of the absorbed dose in various materials.

	Kodak (90 kVp)	I-cat and MDCT (120 kVp)
Bone/air	2.21	1.65
Air/air	1	1
Soft tissue/air	1.09	1.09

3.3 Ratio and propagation of uncertainty between CBCT equipment

The ratio of the mean absorbed dose with propagated uncertainty between Kodak and i-CAT scanners was similar in the lenses of the right and left eye, the right submandibular gland, sublingual gland and the surface of the thyroid. In all other salivary glands, the Kodak showed an absorbed dose up to 1.35 times that for the i-CAT. Nevertheless, the dose absorbed in the middle of the thyroid for the Kodak was approximately half that for the i-CAT (Tab. 4).

Table 4. Ratio of the mean dose values in the most radiosensitive regions with propagated uncertainty at 95% confidence level, between parentheses.

Dosimeter location	MDCT/Kodak	MDCT/I-cat	Kodak/I-cat
Right eye lens*	13.76 (1.76)	17.43 (5.50)	1.27 (0.38)
Left eye lens*	13.79 (1.56)	17.37 (5.56)	1.26 (0.42)
Right parotid Gl	17.61 (2.09)	23.69 (2.94)	1.35 (0.07)
Left parotid Gl	17.95 (2.41)	25.21 (3.94)	1.40 (0.13)
Right submandibular Gl	18.31 (2.03)	24.35 (2.29)	1.33 (0.11)
Left submandibular Gl	15.54 (3.36)	21.87 (7.09)	1.41 (0.54)
Sublingual Gl	18.89 (1.28)	24.65 (2.40)	1.31 (0.15)
Thyroid surface*	150.20 (24.17)	146.54 (29.10)	0.98 (0.21)
Thyroid medium	67.79 (7.93)	30.17 (4.03)	0.45 (0.07)

Gl: Gland.
* Surface dosimeters.

Table 5. Possible applications of CBCT in head and neck diagnosis.

References	Application of CBCT for head and neck
Hodez *et al.* (2011)	Craniofacial trauma
Razafindranaly *et al.* (2016) ; Ruivo *et al.* (2009) ; Hodez *et al.* (2011)	Postoperative assessment of cochlear implantation
Hodez *et al.* (2011) ; Xu *et al.* (2012)	Sinus assessment
Xu *et al.* (2012)	Otologic imaging applications
SEDENTEX CT	Dentomaxillofacial scans protocols

4 Discussion

The use of CBCT for dental and maxillofacial diagnosis and surgical planning is widely diffused among dentists: CBCT scanners provide adequate image quality for dento-maxillofacial examinations while delivering significantly smaller effective doses to the patient (Suomalainen *et al.*, 2009). However, it is important to disseminate scan protocols for the head and neck region to other health specialties. CBCT can provide at least the same information as conventional radiography, digital radiograph and MDCT but in a more comfortable and safer way (Ruivo *et al.*, 2009). As with any guideline, Table 5 is not intended to provide rigid constraints on clinical practice, but a concept of good practice and possible CBCT applications for the head and neck region. For example, CBCT appears to be a useful tool for postoperative assessment of cochlear-implanted adult patients and is comparable to the conventional scanner in determining the scalar position, with lower radiation exposure (Hodez *et al.*, 2011; Ruivo *et al.*, 2009; Razafindranaly *et al.*, 2016). It should be noted that in another investigation (Schegerer *et al.*, 2014), CBCT examination was assessed as well suited for visualizing hard-contrasting objects in the abdomen with relatively low noise and patient dose; nevertheless, for the detection of low-contrast objects at standard tube voltages of approximately 120 kV (p), MDCT should be preferred.

CBCT dose varies substantially depending on the device. The radiation dose of the i-CAT is lower than that of the Mercuray according to a previous study (Ludlow *et al.*, 2006). We found a lower dose for i-CAT than Kodak in all radiosensitive regions, except for the surface and middle of the thyroid. We credit this to the 22 cm FOV of the i-CAT in relation to the 18 cm of the Kodak. In the study by Loubele *et al.* (2009) for example, the highest radiation doses were observed in the two largest acquisition FOVs.

As with any X-ray exposure, CBCT and MDCT can be a risk to the patient. It is essential that any X-ray examination should show a potential benefit to the patient, weighing the total potential diagnostic benefits it produces against the individual detriment that the exposure might cause. The results of this study found a much smaller radiation dose for CBCT protocols than MDCT, similarly to previous studies that identified and justified this difference by the large variation in the parameters and acquisition methods among apparatus (Loubele *et al.*, 2009). Thus, according to the dose of radiation, the results support the choice of CBCT rather than MDCT whenever possible for diagnosis.

In conclusion, radiation dose should be as small as possible for every practice, taking into account image quality and clinical indication and justification. Thus, due to the considerable difference between absorbed doses, highlighting the higher doses in MDCT, it is recommended that the application of CBCT is more widely disseminated, along with further studies to broaden the use criteria.

Acknowledgments

Institute of Radioprotection and Dosimetry (IRD) of Rio de Janeiro for providing the materials used to carry out this study.

Conflicts of interest. The authors declare that they have no conflicts of interest in relation to this article.

The research does not involve human and/or animal participants and therefore, the informed consent form is not required.

References

Chinem LAS, De Souza Vilella B, de Pinho Maurício CL, Canevaro LV, Deluiz LF, de Vasconcellos Vilella O. 2016. Digital orthodontic radiographic set versus cone-beam computed tomography: an evaluation of the effective dose. *Dental Press J. Orthod.* 21(4): 66–72.

Hodez C, Griffaton-Taillandier C, Bensimon I. 2011. Cone-beam imaging: applications in ENT. *Eur. Ann. Otorhinolaryngol. Head Neck Dis.* 128(2): 65–78. https://doi.org/10.1016/j.anorl.2010.10.008.

Loubele M, Bogaerts R, Van Dijck E, Pauwels R, Vanheusden S, Suetens P, Marchal G, Sanderink G, Jacobs R. 2009. Comparison between effective radiation dose of CBCT and MSCT scanners for dentomaxillofacial applications. *Eur. J. Radiol.* 71(3): 461–468. https://doi.org/10.1016/j.ejrad.2008.06.002.

Ludlow JB, Davies-Ludlow LE, Brooks SL, Howerton WB. 2006. Dosimetry of 3 CBCT devices for oral and maxillofacial radiology: CB Mercuray, NewTom 3G and i-CAT. *Dentomaxillof. Radiol.* 35(4): 219–26. https://doi.org/10.1259/dmfr/14340323.

Ludlow JB, Walker C. 2013. Assessment of phantom dosimetry and image quality of I-CAT FLX cone-beam computed tomography. *Am. J. Orthod. Dentofacial Orthop.* 144(6): 802–817. https://doi.org/10.1016/j.ajodo.2013.07.013.

Razafindranaly V, Truy E, Pialat JB, Martinon A, Bourhis M, Boublay N, Faure F, Ltaief-Boudrigua A. 2016. Cone beam CT versus multislice CT: radiologic diagnostic agreement in the postoperative assessment of cochlear implantation. *Otol. Neurotol.* 37(9): 1246–1254. https://doi.org/10.1097/MAO.0000000000001165.

Ruivo J, Mermuys K, Bacher K, Kuhweide R, Offeciers E, Casselman JW. 2009. Cone beam computed tomography, a low-dose imaging technique in the postoperative assessment of cochlear implantation. *Otol. Neurotol.* 30(3): 299–303. https://doi.org/10.1097/MAO.0b013e31819679f9.

Schegerer AA, Lechel U, Ritter M, Weisser G, Fink C, Brix G. 2014. Dose and image quality of cone-beam computed tomography as compared with conventional multislice computed tomography in abdominal imaging. *Invest. Radiol.* 49(10): 675–684. https://doi.org/10.1097/RLI.0000000000000069.

Sun R, Cai Y, Yuan Y, Hong Zhao J. 2017. The characteristics of adjacent anatomy of mandibular third molar germs: a CBCT study to assess the risk of extraction. *Sci. Rep.* 7(1): 1–7. https://doi.org/10.1038/s41598-017-14144-y.

Suomalainen A, Kiljunen T, Käser Y, Peltola J, Kortesniemi M. 2009. Dosimetry and image quality of four dental cone beam computed tomography scanners compared with multislice computed tomography scanners. *Dentomaxillof. Radiol.* 38(6): 367–378. https://doi.org/10.1259/dmfr/15779208.

Xu J, Reh DD, Carey JP, Mahesh M, Siewerdsen JH. 2012. Technical assessment of a cone-beam CT scanner for otolaryngology imaging: image quality, dose, and technique protocols. *Med. Phys.* 39(8): 4932–4942. https://doi.org/10.1118/1.4736805.

Cite this article as: Oliveira PLE, Starling CR, Maurício CLP, Guedes FR, Visconti MA, Ruellas ACO. 2021. Ionizing radiation and its considerations in imaging diagnosis: comparison of absorbed dose between cone beam computed tomography and multi-detector computed tomography in the head and neck. *Radioprotection* 56(2): 111–115